JOURNAL OF SOLID STATE CHEMISTRY 54, 282–290 (1984)

Preparation of Lithium Molybdenum Oxide Bronzes by a Temperature Gradient Flux Growth Technique

W. H. McCARROLL AND M. GREENBLATT*

Department of Chemistry, Rutgers, The State University of New Jersey, New Brunswick, New Jersey 08903

Received December 9, 1983; in revised form May 14, 1984

Single crystals of the violet–red $Li_{0.9}Mo_6O_{17}$, violet–blue $Li_{0.32}MoO_3$, and the new blue $Li_{0.04}MoO_3$ bronzes have been grown by a temperature gradient flux growth method in evacuated quartz ampoules. Optimal growth conditions determined for each of the phases are reported. $Li_{0.9}Mo_6O_{17}$ is monoclinic, and a quasi-two-dimensional metallic conductor at room temperature, similar to $K_{0.9}Mo_6O_{17}$ · $Li_{0.04}MoO_3$ appears to be a new intercalation compound of MoO_3.

Introduction

Fused salt electrolysis has been the principal means of growing single crystals of alkali molybdenum bronzes that are suitable for electrical and magnetic measurements (*1–4*). There are no reports of the successful use of vapor transport methods for molybdenum bronzes and flux growth appears to have been applied only to the tungsten bronzes (*5, 6*). Attempts were made in this laboratory to grow lithium molybdenum bronze crystals by vapor transport, using iodine as transport agent in the hope that LiI, the most covalent of the alkali halides, might successfully transport lithium. Although these attempts were unsuccessful in that no bronzes were formed by transport, the melts formed under the conditions used yielded highly crystalline reduced products. This observation has led to a more intensive investigation of the flux growth of oxide bronzes in the Li–Mo–O system, the results of which are reported here.

Experimental

The Li_2MoO_4 used in these experiments, which was obtained from ROC/RIC and had a stated purity of 98%, was doubly recrystallized before use. Reagent grade MoO_3, obtained from Baker Chemicals was normally dried at 160°C before use but was ignited at 450°C if it had a slight bluish tinge. MoO_2, also obtained from ROC/RIC, stated purity 99.9%, was washed several times with alternate portions of hot, dilute HCl, water, and ammonia to remove traces of molybdenum blue. All reactions were run in evacuated, sealed ampoules made from quartz tubing (11 mm i.d.) that had been soaked for several hours in aqua regia. Stoichiometric quantities of reactants were weighed out according to the equation

$$n\mathrm{Li_2MoO_4} + 2(1-n)\mathrm{MoO_3} + n\mathrm{MoO_2} \rightarrow 2\mathrm{Li}_n\mathrm{MoO_3} \quad (0.05 \leq n \leq 0.60),$$

* Author to whom correspondence should be addressed.

0022-4596/84 $3.00

to yield a total charge of 10 g. This was mixed thoroughly by grinding in an agate mortar and pressed into three 0.375-in.-diameter pellets that were flamed lightly *in vacuo* to remove absorbed moisture before sealing off in 15-cm-long ampoules at a pressure of 2×10^{-2} Torr. The reactions were run in a Mellen two-zone, 2-in.-diameter tube furnace, with each zone controlled by a Eurotherm controller. The temperature at any given point in the working zones was controlled within ±3°C during the course of a run. Usually a brace of four ampoules was placed in the furnace for a given run. The charge, which was 6.5- to 7-cm long was placed at the end of the ampoule that was to be placed in the hot zone.

The standard procedure involved an initial heating, designed to yield a polycrystalline initial product or mixture of products, which was carried out for 3 days (usually) at a given setting of the temperatures in the two zones, followed by the final or crystallization reaction which was carried out at somewhat higher (60–90°C) temperatures for 7 to 10 days. Runs were terminated by allowing the ampoules to cool at a rate of approximately 1.5°C/min for about an hour before removing them from the furnace. Typical reaction parameters are given in Table I.

Phases formed were identified principally by X-ray powder diffractometry although occasionally photographic methods were employed. Filtered copper radiation was used throughout. Separated single-phase samples were chemically analyzed for lithium and molybdenum by using atomic absorption and plasma emission spectroscopy. Typically, reduced phases could be separated from the matrix by leaching with either hot 5% potassium carbonate or hot 5% sodium dihydrogen phosphate alternated with 2 *M* hydrochloric acid, until the solutions obtained were colorless. If necessary, mechanical separations followed. Some attack of the silica ampoule was evident where melting had occurred and siliceous material, if present in the purified product, could be removed in most instances by washing with hot 10% hydrofluoric acid without serious loss of the reduced phase.

Results for Li_nMoO_3, $0.05 \leq n \leq 0.60$

In the discussion that follows the chemical formula Li_nMoO_3 will refer to nominal starting compositions made up from stoichiometric quantities of lithium molybdate, molybdenum(IV) oxide, and molybdenum(VI) oxide while Li_xMoO_3 will refer to the violet–blue bronzes previously prepared by Reau *et al.* (*7*) that were reported to have a range of stoichiometry, with $0.31 \leq x \leq 0.39$. $Li_{0.04}MoO_3$ is used to designate a previously unreported reduced oxide.

The system Li_nMoO_3 was investigated over the range $0.05 \leq n \leq 0.60$. The particular phases formed depend not only upon the value of n but also upon the range of temperatures to which various portions of the reacting mix were subjected. Growth of the phases of interest appeared to be optimized by preheating the charge several days at a temperature well below melting (i.e., around 550–580°C; both zones kept at the same temperature) followed by additional heating in a gradient in which the hot end of the ampoule was at approximately 640°C and the cold end at about 590°C. Without preheating, the size and perfection of the reduced crystalline phases were generally found to have diminished. Higher temperatures may also result in degradation of crystal quality or the formation of unwanted binary oxides. Cooling of the ampoules at the end of a run for about 1 hr before removing them from the furnace served to prevent their cracking and oxidation, which sometimes occurred when they were quenched from the growth temperature. Crystal growth was complete prior to this cooling process as observed in some of

TABLE I

SUMMARY OF PHASES FORMED FOR VARIOUS GROWTH CONDITIONS

Sample	n	T_i (°C)	t_i	T_0 (°C)	T_7 (°C)	T_{10} (°C)	T_{15} (°C)	t_f	Reduced product and comment
II-109	0.05	580	3	637	637	637	637	10	No melting; $Li_{0.04}MoO_3$
II-108	0.10	580	3	637	637	637	637	10	No melting; $Li_{0.04}MoO_3$
II-27	0.15	575	3	641	623	608	588	7	No melting; $Li_{0.04}MoO_3$
II-45	0.20	575	3	641	625	610	588	7	No melting; $Li_{0.04}MoO_3$ in cold end. γ-Mo_4O_{11} and $Li_{0.9}Mo_6O_{17}$ in hot end
III-34	0.23	570	3	644	627	614	595	7	Partial melting; mainly $Li_{0.9}Mo_6O_{17}$ in cold end + some $Li_{0.04}MoO_3$, γ-Mo_4O_{11} also found in hot end
I-104	0.26	576	3	644	625	607	588	7	As in III-34 but better quality $Li_{0.9}Mo_6O_{17}$
II-28	0.26	575	4	643	625	609	590	10	As in III-34 but better quality $Li_{0.9}Mo_6O_{17}$ crystals. Many plates 4–7 mm in diameter
III-41	0.26	575	3	668	650	635	620	10	Same phases present as in II-28 but considerably poorer quality crystals; more intergrowth. Some Li_xMoO_3 needles also observed
III-33	0.26	—	—	644	625	610	590	7	No preheat. Same phases as in II-28 but $Li_{0.9}Mo_6O_{17}$ crystals smaller and more intergrown
III-20	0.30	575	3	640	623	610	588	10	Phase distribution similar to that of II-28 but with more extensive melting. Crystals of $Li_{0.9}Mo_6O_{17}$ are 3–5 mm in diameter
II-26	0.33	575	3	641	623	608	588	7	Crystals of $Li_{0.9}Mo_6O_{17}$ and $Li_{0.04}MoO_3$ in colder region. Li_xMoO_3, γ-Mo_4O_{11}, and MoO_2 crystals in hotter regions
III-36	0.36	570	3	644	627	614	595	7	Similar to II-26. Li_xMoO_3 grows as fine needles intermixed with MoO_2. $Li_{0.9}Mo_6O_{17}$ dominant phase
II-106	0.40	565	3	636	620	605	586	10	Melting occurs throughout. Large platelet crystals of Li_xMoO_3 form which are 1 × 4 × 5 mm in hot end. Large prisms of Li_xMoO_3 crystals 1 × 1 × 5–7 in 600°C region
III-42	0.40	575	3	668	650	635	620	10	Principal reduced phase is Li_xMoO_3 in form of fine, thin purple needles 2–4 mm long
III-9	0.50	575	3	642	625	612	592	7	Dominant reduced phase is Li_xMoO_3 in the form of fine needles, some very small MoO_2 crystals <0.5 mm
III-13	0.60	575	3	640	624	610	590	7	MoO_2 is only reduced phase observed

Note. T_i = the initial temperature used to heat the entire charge. t_i,t_f = the time in days for the initial and final heating conditions, respectively. T_0, T_7, T_{10}, T_{15} are temperatures across the length of the ampoule during t_f; subscripts represent distances in centimeters measured from the hot end.

the experiments where the ampoules were quenched to room temperature at the termination of a run. The results are summarized briefly in Table I and the discussion which follows refers to the gradient conditions outlined above unless otherwise stated.

For n = 0.05 and 0.10 no signs of melting are evident. The pellets are coated with blue dendritic flakes while their interior is predominantly MoO_3 with small blue needles mixed in as a minor phase. The interior and exterior blue phases have identical X-ray powder diffraction patterns. The composition appears to be close to $Li_{0.04}MoO_3$ based on analysis of several different samples of the dendritic material. The blue needles are 1–2 mm long on average.

For n = 0.15 again there is no melting,

however, in addition to the blue dendritic flakes of $Li_{0.04}MoO_3$, some $Li_2Mo_4O_{13}$ is also present as shown by the X-ray powder diffraction pattern.

For starting composition $Li_{0.20}MoO_3$, the sample has maintained its pelletized shape, albeit with considerable shrinkage due to sintering and incipient melting. Although uniformly blue on the outside, the pellets are a mixture of phases in the interior. For the portion of the charge in the 625–630°C region the principal phase is $Li_{0.04}MoO_3$ in the form of thin rods 2 to 3 mm long. $Li_{0.9}Mo_6O_{17}$ and γ-Mo_4O_{11} (the high-temperature form) are also present as small crystals (less than 1 mm in largest dimension) and polycrystalline aggregates. The predominant reduced phase found in the region heated between 630 and 641°C appears to be γ-Mo_4O_{11} but $Li_{0.9}Mo_6O_{17}$ and $Li_{0.04}MoO_3$ are also present. $Li_2Mo_4O_{13}$ is also present throughout the sample.

When n is between 0.23 and 0.33 both melting and flow toward the cooler end of the ampoule take place, with the amount of flow increasing with n. At $n = 0.23$ the melted region contains principally blue crystals of $Li_{0.04}MoO_3$ intermixed with small violet–red platelets of $Li_{0.9}Mo_6O_{17}$, 2–3 mm in largest dimension. For $n = 0.26$ flow takes place down to where the temperature was about 610°C about 2 cm beyond the initial position of the charge; for $n = 0.33$ the melt extended almost to the end of the ampoule where the temperature was about 590°C. However, the position of the original charge is clearly evident. In the region of 595–625°C, the reduced phases obtained are $Li_{0.04}MoO_3$ and $Li_{0.9}Mo_6O_{17}$ with the amount of the former decreasing as n increases. The growth of $Li_{0.9}Mo_6O_{17}$ appears to be maximized in the region $n = 0.26$–0.33 with plates typically in the diameter region 3–6 mm, and some as large as 8–10 mm. For $n = 0.26$ some fine purple needles are also found whose X-ray diffraction pattern corresponds to that previously found for the monoclinic bronze Li_xMoO_3 ($0.31 \leq x \leq 0.39$) (*7*). Above 630°C the principal reduced phase is again γ-Mo_4O_{11} but for $n = 0.33$ significant amounts of fine Li_xMoO_3 and polycrystalline MoO_2 are also found.

At $n = 0.36$ a similar regimen exists except that the relative amount of $Li_{0.9}Mo_6O_{17}$ and $Li_{0.04}MoO_3$ is markedly decreased in both quality and quantity, while the amounts of Li_xMoO_3 and MoO_2 increase.

At $n = 0.40$ the sample melts completely and flows throughout the ampoule. In the coldest regions (586–620°C) the dominant phase is now Li_xMoO_3. In addition to the fine needles of this phase previously observed, several large prisms (5–7 mm in length and 1–2 mm thick) are found, principally in the 600°C region, and surprisingly large platelet crystals ($1 \times 4 \times 5$ mm) of Li_xMoO_3 are also found in the 610–620°C region. Some MoO_2 is also evident as very small crystals mixed in with the mass of fine needles of Li_xMoO_3.

At $n = 0.50$ complete melting of the sample and flow throughout the ampoule again occurs. The dominant reduced phase is Li_xMoO_3 in the form of fine needles; some very small MoO_2 crystals (<0.5 mm) are also present. The principal nonreduced phase in the melt is $Li_4Mo_5O_{17}$. A smaller quantity of $Li_2Mo_4O_{13}$ is also evident. For $n = 0.60$, melting is complete and the position of the original charge is no longer evident. The only reduced phase is MoO_2 which grows in the form of prisms 2–3 mm long that are particularly noteworthy for their smooth, highly reflecting, well-formed faces (Fig. 1d).

Discussion

The flux growth technique has been used successfully to prepare large single crystal specimens of $Li_{0.32}MoO_3$, $Li_{0.9}Mo_6O_{17}$, and $Li_{0.04}MoO_3$. Figures 1a–d show typical examples of crystal sizes and morphologies

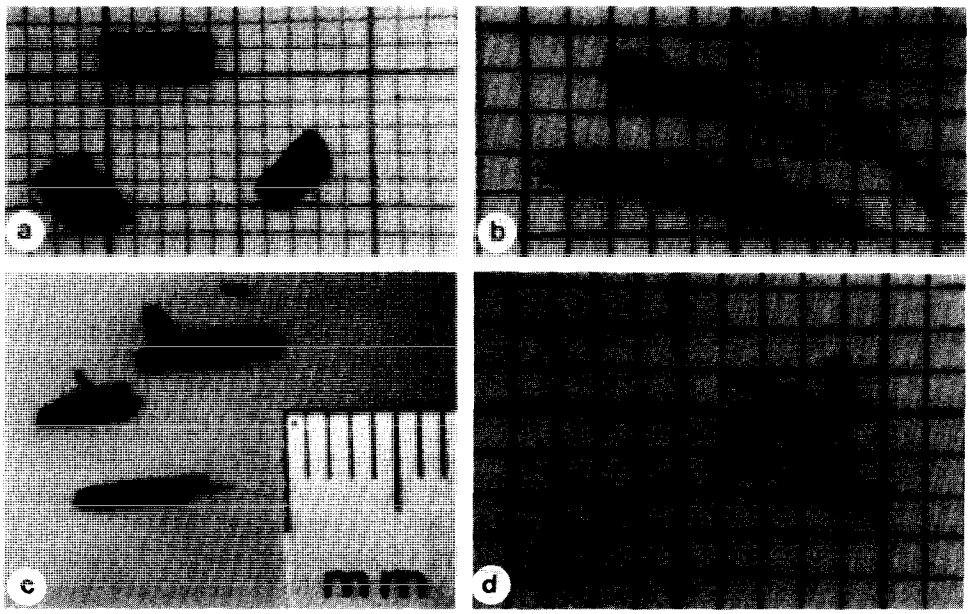

FIG. 1. Crystals of (a) $Li_{0.9}Mo_6O_{17}$, (b) $Li_{0.04}MoO_3$, (c) Li_xMoO_3, (d) MoO_2. The grid spacings in a–d are in millimeters.

obtained. The optimum starting compositions of the charge Li_nMoO_3 for the growth of $Li_{0.9}Mo_6O_{17}$ appear to be in the range $0.26 \leq n \leq 0.33$ while crystals of Li_xMoO_3 could be isolated in pure form only for $n = 0.40$ and $n = 0.50$. $Li_{0.04}MoO_3$ grows best for $0.23 \leq n \leq 0.30$. The size and quality of the crystals does not appear to be markedly dependent upon the cooling rate at the end of the run. However, we intend to look at this aspect more closely in the future.

$Li_{0.9}Mo_6O_{17}$ was first prepared by Reau *et al.* using a solid state reaction (*7*). Its crystal structure is not known although Gatehouse *et al.* did some single crystal X-ray diffraction studies which showed that its space group is different from that of the Na and K analogs (*8*). Four probe resistivity measurements down to liquid-helium temperatures show that $Li_{0.9}Mo_6O_{17}$ displays metallic conductivity and that the conductance is highly anisotropic. The room-temperature resistivity, measured in the direction parallel to the plate axis, is 9.5×10^{-3} and 2.47 Ω cm perpendicular to that axis. Thus the conductivity at room temperature is ~250 times greater in the easy direction (*ab* plane) than along the direction parallel to the *c* axis. This highly anisotropic behavior is similar to that reported for $K_{0.9}Mo_6O_{17}$ (*9*) whose recently determined structure (*10*) is consistent with such two-dimensional behavior. A more detailed presentation of the electrical properties of $Li_{0.9}Mo_6O_{17}$ will be given elsewhere (*11*). $K_{0.9}Mo_6O_{17}$ is trigonal and the strong lines of the powder pattern of $Li_{0.9}Mo_6O_{17}$ can be indexed on the basis of a similar unit cell (*7*). However, weak but clearly discernible lines in the low-angle region of a Debye–Scherrer photograph coupled with the splitting of some higher angle lines can only be accounted for on the basis of a monoclinic unit cell. This observation is in agreement with the single crystal patterns of the lithium compound observed by Gatehouse *et al.* (*8*). Their lattice parameters differ somewhat from those reported by Reau *et*

al. (*7*). This might be taken as evidence for a small range of nonstoichiometry in $Li_{0.9}Mo_6O_{17}$. However, our chemical analysis of several samples prepared from charges covering a wide range of lithium content gives values for Li between 0.87 and 0.93 per Mo_6O_{17} unit (See Table II). Further, we were unable to detect any change in the lattice parameters for all of the analyzed samples. Thus it appears safe to assume that any range of nonstoichiometry, if indeed one exists, is quite small. Our X-ray data yields a considerably better fit for Gatehouse's (*8*) unit cell parameters (a = 9.482 Å, b = 5.521 Å, c = 12.737 Å, β = 90.59°) and these have been used to index the X-ray powder diffraction pattern given in Table III.

Li_xMoO_3 is a semiconductor (*4*) whose crystal structure is not known. Although Li_xMoO_3 was observed throughout the range $0.26 \leq n \leq 0.50$, pure samples of this phase were isolated only for n = 0.40 and 0.50. Interestingly, chemical analysis shows that both samples have a composition close to $Li_{0.32}MoO_3$ (see Table II). This observation coupled with the fact that Strobel and Greenblatt (*4*) found that x = 0.33 for an electrolytically prepared sample, indicates that the range of homogeneity of this phase is considerably less than that reported previously (*7*). Further, we find no variation in interplanar spacing for specimens of this phase prepared from charges with $0.26 \leq n \leq 0.50$. However, the X-ray diffraction pattern for each of our two pure samples of Li_xMoO_3 shows the compound to have a somewhat larger unit cell than that reported by Reau and co-workers (*7*) for a sample of unspecified lithium content.

The blue phase, $Li_{0.04}MoO_3$, has not been reported previously. It has not been observed in the ternary Li_xMoO_3 products prepared by the topotactic reduction of MoO_3 either with n-butyl lithium or electrochemically (*13*). The results of chemical

TABLE II

RESULTS OF CHEMICAL ANALYSIS

Sample No.	Charge composition	Phase type isolated	%Li (obs.)	%Mo (obs.)	Calcd. formula
III-34B-1	$Li_{0.23}MoO_3$	$Li_{0.04}MoO_3$	0.211		$Li_{0.043}MoO_3$[a]
II-14A	$Li_{0.26}MoO_3$	$Li_{0.04}MoO_3$	0.18	66.6	$Li_{0.037}MoO_3$
III-20C-1	$Li_{0.30}MoO_3$	$Li_{0.04}MoO_3$	0.210	66.5	$Li_{0.043}MoO_3$
III-20C-2	$Li_{0.30}MoO_3$	$Li_{0.04}MoO_3$	0.210		$Li_{0.043}MoO_3$[a]
II-26A-1	$Li_{0.33}MoO_3$	$Li_{0.04}MoO_3$	0.204	66.7	$Li_{0.042}MoO_3$
II-106A-1	$Li_{0.40}MoO_3$	Li_xMoO_3	1.52	65.8	$Li_{0.32}MoO_{2.98}$
III-9	$Li_{0.50}MoO_3$	Li_xMoO_3	1.53	65.7	$Li_{0.32}MoO_{2.99}$
III-35B	$Li_{0.26}MoO_3$	$Li_{0.9}Mo_6O_{17}$	0.727	67.80	$Li_{0.89}Mo_6O_{16.7}$
III-18B	$Li_{0.26}MoO_3$	$Li_{0.9}Mo_6O_{17}$	0.716		$Li_{0.88}Mo_6O_{17}$[b]
II-28-4	$Li_{0.26}MoO_3$	$Li_{0.9}Mo_6O_{17}$	0.723		$Li_{0.89}Mo_6O_{17}$[b]
III-18B-1	$Li_{0.26}MoO_3$	$Li_{0.9}Mo_6O_{17}$	0.722		$Li_{0.89}Mo_6O_{17}$[b]
III-20D-1	$Li_{0.30}MoO_3$	$Li_{0.9}Mo_6O_{17}$	0.726		$Li_{0.89}Mo_6O_{17}$[b]
II-107A-1	$Li_{0.33}MoO_3$	$Li_{0.9}Mo_6O_{17}$	0.730	67.4[c]	$Li_{0.90}Mo_6O_{17.0}$
II-107A-2	$Li_{0.33}MoO_3$	$Li_{0.9}Mo_6O_{17}$	0.754	67.6	$Li_{0.93}Mo_6O_{16.8}$
II-26/104	$Li_{0.33}MoO_3$	$Li_{0.9}Mo_6O_{17}$	0.750		$Li_{0.92}Mo_6O_{17}$[b]
III-36B	$Li_{0.36}MoO_3$	$Li_{0.9}Mo_6O_{17}$	0.740		$Li_{0.91}Mo_6O_{17}$[b]

[a] Chemical formula calculated on the basis of an MoO_3 stoichiometry.

[b] Chemical formula calculated on basis of Mo_6O_{17} stoichiometry.

[c] Theoretical %Mo for $Li_{0.9}Mo_6O_{17}$ is 67.4%.

TABLE III

X-RAY POWDER DIFFRACTION PATTERN OF $Li_{0.9}Mo_6O_{17}$; MONOCLINIC INDEXING[a]

d_{obs}	d_{calc}	I/I_0	hkl
7.65	7.64	1	$10\bar{1}$, 101
5.29	5.29	1	$10\bar{2}$, 102
4.76	4.76	2	110, 200
4.25	4.25	3	003
3.82	3.82	100	$11\bar{2}$, $20\bar{2}$, 112
3.601	3.597	3	210
3.473	3.461	1	$21\bar{1}$, 211
3.367	3.365	1	013
3.192	3.181	3	004, $11\bar{3}$, $20\bar{3}$
3.167	3.162	5	113, 300
3.139	3.136	5	203, $21\bar{2}$, 212
3.018	3.018	<1	$10\bar{4}$, 104
2.755	2.758	17	020, 014, $21\bar{3}$
2.748	2.738	23	213, 310
2.659	2.654	30	204, $11\bar{4}$, 120
2.633	2.636	10	114, 204
2.549	2.548	2	$30\bar{3}$, 005
2.450	2.454	1	$10\bar{5}$, 105, $12\bar{2}$, 122
2.347	2.345	2	$22\bar{1}$, 221, 404
2.256	2.253	3	$30\bar{4}$, $20\bar{5}$, $11\bar{5}$, $12\bar{3}$
2.237	2.236	10	123, 115, $22\bar{2}$, 205, 304, 222, $40\bar{2}$
2.215	2.214	3	402
2.144	2.147	1	$41\bar{1}$, 411
2.124	2.123	1	006
2.080	2.081	1	$31\bar{4}$, $21\bar{5}$, 024, $22\bar{3}$, 320, $40\bar{3}$, $10\bar{6}$, $22\bar{3}$
2.071	2.068	1	215, 314, 106, $41\bar{2}$
2.054	2.053	1	412, $32\bar{1}$, 321
1.915	1.912	7	$22\bar{4}$
1.906	1.904	17	224
1.820	1.821	2	$50\bar{2}$, 216, 031, 003
1.779	1.781	2	107, $42\bar{1}$, 421, $51\bar{1}$
1.736	1.737	13	$13\bar{2}$, $50\bar{3}$, 132, 225, 324, $42\bar{2}$
1.731	1.731	10	512, 017
1.699	1.701	3	$20\bar{7}$, $11\bar{7}$, $23\bar{1}$, 117
1.684	1.684	12	$31\bar{6}$, 026
1.672	1.672	5	316
1.659	1.659	2	133, $42\bar{3}$, 126, $23\bar{2}$, $51\bar{3}$
1.652	1.653	2	232, 126, 423
1.590	1.591	5	034, $23\bar{3}$, 008, 330, $22\bar{6}$, $40\bar{6}$, 233

[a] Indexed using single crystal parameters of Gatehouse *et al.* (*8*) $a = 9.482$ Å, $b = 5.521$ Å, $c = 12.737$ Å, $\beta = 90.59°$.

analysis of $Li_{0.04}MoO_3$ indicate that the lithium content is relatively constant and very close to 0.04 (see Table II). The acidity of the material is evidenced by the fact that it is rapidly decomposed by a hot 5% potassium carbonate solution which leaves an inhomogeneous greyish, amorphous residue. The crystals of $Li_{0.04}MoO_3$ appear to be twinned, and we were unable to determine the lattice parameters unambigously using Weissenberg and precession photography. However, the lattice obviously bears a close resemblance to that of MoO_3 as shown by the comparison of the X-ray powder diffraction patterns of $Li_{0.04}MoO_3$ and MoO_3 given in Table IV. The similarity of the patterns is noteworthy. However, there are small but significant shifts in the d spacings, and marked differences in the intensity data. These are reasonably reproducible from sample to sample, indicating that the intensity difference is not a preferred orientation effect; an observation which is confirmed by powder photography.

These observations suggest that a small but reproducible amount of lithium intercalation has taken place under the conditions of these experiments. Further, the compound is a moderately good conductor of electricity while MoO_3 is an insulator. Four probe resistivity measurements at room temperature yield a resistivity value of ~2 Ω cm. Cooling the sample increases the resistivity considerably, which indicates semiconductivity. A qualitative measurement of the sign of the Seebeck coefficient is consistent with p-type majority carriers. More extensive measurements of the transport properties are planned.

It is noteworthy that $Li_2Mo_4O_{13}$ is found throughout the samples for $0.15 \leq n \leq 0.50$ where bronze formation is observed. Electrolytic growth of alkali molybdenum bronze single crystals on the cathode has been successful only in a narrow range of melt composition, corresponding to the starting phase $A_2Mo_4O_{13}$ (*4*). Subsequent

TABLE IV

COMPARISON OF THE X-RAY POWDER DIFFRACTION PATTERN OF $Li_{0.042}MoO_3$ WITH THAT OF MoO_3

$Li_{0.042}MoO_3$		MoO_3(PDF 5-508)		
d_{obs}	I/I_0	d_{obs}	I/I_0	hkl
6.94	58	6.93	34	0.20
4.15	3	—	—	—
3.84	1	3.81	82	110
3.52	13	—	—	—
3.469	100	3.468	61	040
3.342	10	—	—	—
3.226	10	3.260	100	021
—	—	3.006	13	130
2.876	2	—	—	—
2.836	1	—	—	—
—	—	2.702	19	101
2.633	5	2.655	35	111
—	—	2.607	6	140
2.564	1	2.527	12	041
2.335	3	2.332	12	131
2.316	45	2.309	31	060
—	—	2.271	18	150
2.220	5	—	—	—
2.196	3	—	—	—
—	—	2.131	9	141
—	—	1.996	4	160
1.979	5	1.982	13	200
1.955	1	1.960	17	061
1.867	3	—	—	—
—	—	1.849	21	002
1.814	1	1.821	11	230
—	—	1.771	5	170
—	—	1.756	5	161
1.737	1	1.733	17	080
1.729	1	—	—	—
1.710	1	—	—	—
—	—	1.693	8	221
1.665	1	1.663	13	112
1.654	2	—	—	—
1.644	3	—	—	—
1.636	4	1.631	13	042
1.608	2	—	—	—
1.598	4	1.597	15	171
1.581	2	1.587	6	180
1.569	4	1.569	16	081

experiments produced Li_xMoO_3 crystals throughout the melt by slow cooling of electrolyzed Li_2MoO_4–MoO_3 melts with bronze formation optimized for a starting composition close to $Li_2Mo_4O_{13}$ (*12*). Thus it appears that the presence of $Li_2Mo_4O_{13}$ is essential for bronze formation. It was suggested before (*4*) that the formation of bronzes occur due to the presence of the edge-sharing molybdenum octahedra in the melt as are found in $Li_2Mo_4O_{13}$.

Conclusions

The temperature gradient flux technique has been used successfully to yield large crystals of lithium molybdenum bronzes: $Li_{0.9}Mo_6O_{17}$, $Li_{0.32}MoO_3$, and $Li_{0.04}MoO_3$. Stoichiometric mixtures of Li_2MoO_4–MoO_3–MoO_2 made up to the nominal starting composition Li_nMoO_3 with $0.05 \leq n \leq 0.60$ were enclosed in evacuated quartz ampoules and heated in a two-zone furnace. The particular phases formed and the quality of crystals depend on the value of n and the temperature gradient of the reaction mixture. The growth of $Li_{0.9}Mo_6O_{17}$ is optimized for $n = 0.26$–0.33. The largest crystals of $Li_{0.32}MoO_3$ have been grown at $n = 0.40$ and growth conditions for $Li_{0.04}MoO_3$ are optimal when $0.23 \leq n \leq 0.30$.

$Li_{0.9}Mo_6O_{17}$ is monoclinic and is a quasi-two-dimensional metallic conductor at room temperature, similar to the potassium analog $K_{0.9}Mo_6O_{17}$. $Li_{0.04}MoO_3$ is a *p*-type semiconductor.

$Li_2Mo_4O_{13}$ appears to be a requisite phase in the reaction mixture for formation of the bronzes $Li_{0.9}Mo_6O_{17}$ and Li_xMoO_3. In addition it significantly promotes crystal growth of $Li_{0.04}MoO_3$.

Acknowledgments

We acknowledge Dr. S. DiGregorio and B. Eiberger for their initial vapor transport experiments on the Li–Mo–O system. We thank R. Neifeld and Professor M. Croft of the Physics Department for their assistance with the resistivity measurements and illuminating discussions on the physical properties of the phases studied. We thank E. Wang for single crystal X-ray diffrac-

tion measurements, and Dr. K. V. R. Chary for technical assistance. The work received support from the National Science Foundation–Solid State Chemistry Grant DMR-81-15977. W. H. M. gratefully acknowledges support under the Small College Faculty Research Participation Program of NSF.

References

1. A. WOLD, W. KUNNMANN, R. J. ARNOTT, AND A. FERRETTI, *Inorg. Chem.* **3,** 545 (1964).
2. G. H. BOUCHARD, JR., J. PERLSTEIN, AND M. J. SIENKO, *Inorg. Chem.* **6,** 1682 (1967).
3. T. I. DROBASHEVA, V. P. ZUEVA, AND V. I. SPITSYN, *Russ. J. Inorg. Chem.* **25,** 941 (1980).
4. P. STROBEL AND M. GREENBLATT, *J. Solid State Chem.* **36,** 331 (1981).
5. M. E. STRAUMANIS, *J. Amer. Chem. Soc.* **71,** 679 (1949).
6. E. O. BRIMM, J. C. BRANTLEY, J. H. LORENZ, AND M. H. JELLINEK, *J. Amer. Chem. Soc.* **73,** 5427 (1951).
7. J. M. REAU, C. FOUASSIER, AND P. HAGENMULLER, *J. Solid State Chem.* **1,** 326 (1970).
8. B. M. GATEHOUSE, D. J. LLOYD, AND B. K. MISKIN, *NBS Spec. Publ. (U.S.)* 364; "Proceedings, 5th Materials Research Symposium," Vol. 15 (1972).
9. R. BUDER, J. DEVENYI, J. DUMAS, J. MARCUS, J. MERCIER, C. SCHLENKER, AND H. VINCENT, *J. Phys. (Paris) Lett.* **43,** L-59 (1982).
10. H. VINCENT, M. GHEDIRA, J. MARCUS, J. MERCIER, AND C. SCHLENKER, *J. Solid State Chem.* **47,** 113 (1983).
11. M. GREENBLATT, W. H. MCCARROLL, R. NEIFELD, M. CROFT, AND J. WASZCZAK, *Solid State Comm.*, in press.
12. K. RAVINDRAN NAIR, E. WANG, AND M. GREENBLATT, *J. Solid State Chem.*, in press.
13. J. O. BESENHARD AND R. SCHOLLHORN, *J. Power Sources* **1,** 267 (1976).